

High Energy X-ray spectra of Seyferts and Unification schemes for AGN

Matthew Middleton¹, Chris Done¹ and Nick Schurch¹

¹*Department of Physics, University of Durham, South Road, Durham DH1 3LE, UK*

ABSTRACT

The Unified Model of AGN predicts the sole difference between Seyfert 1 and Seyfert 2 nuclei is the viewing angle with respect to an obscuring structure around the nucleus. High energy photons above 20 keV are not affected by this absorption if the column is Compton thin, so their 30–100 keV spectra should be the same. However, the observed spectra at high energies appear to show a systematic difference, with Seyfert 1's having $\Gamma \sim 2.1$ whereas Seyfert 2's are harder with $\Gamma \sim 1.9$. We estimate the mass and accretion rate of Seyferts detected in these high energy samples and show that they span a wide range in L/L_{Edd} . Both black hole binary systems and AGN show a correlation between spectral softness and Eddington fraction, so these samples are probably heterogeneous, spanning a range of intrinsic spectral indices which are hidden in individual objects by poor signal-to-noise. However, the mean Eddington fraction for the Seyfert 1's is higher than for the Seyfert 2's, so the samples are consistent with this being the origin of the softer spectra seen in Seyfert 1's. We stress that high energy spectra alone are not necessarily a clean test of Unification schemes, but that the intrinsic nuclear properties should also change with L/L_{Edd} .

Key words: accretion, accretion discs, black hole – Galaxies: Seyfert

1 INTRODUCTION

The simplest version of the Unification model of Antonucci & Miller (1985) is that the central engine (black hole, its accretion disc and broad line region: BLR) are the same in all AGN, but that this is embedded in an obscuring torus. The nucleus is seen directly only for inclination angles which do not intersect this material, giving the classic Seyfert 1 AGN signature of a strong and variable UV/X-ray continuum and broad emission lines. Conversely, where the obscuration is in the line of sight, these features are hidden, and the presence of an AGN can only be inferred from the high excitation lines produced in the narrow line region on much larger scales (Seyfert 2's). A key piece of evidence for this scenario is the detection of polarized broad emission lines in classic Seyfert 2 galaxies (most notably in NGC 1068), showing that the BLR is present, but can only be seen via scattered light (e.g. Antonucci & Miller 1985; Tran 1995; Heisler et al. 1997). This scattering medium filling the 'hole' in the torus is also detected in transmission in Seyfert 1's through the partially ionised absorption signatures seen in soft X-rays (e.g. Blustin et al 2005).

The intrinsic X-ray spectrum of a type 1 AGN can be well described by a power law (of photon spectrum $N(E) \propto E^{-\Gamma}$) together with its Compton reflection from the optically thick accretion disc and/or torus (e.g. Nandra & Pounds 1994). Again, the Unified models are supported by

X-ray observations, which show that this intrinsic spectrum is substantially suppressed at low energies due to absorption in Seyfert 2's (Awaki et al 1991; Smith & Done 1996; Turner et al 1997; Bassani et al 1999; Cappi et al 2006). However, the strong energy dependence of photoelectric absorption means that this is unlikely to affect samples above 10 keV for columns which are not Compton thick, yet high energy experiments show that the intrinsic spectra of Seyfert 2 galaxies are systematically harder ($\Gamma \sim 1.9 - 2$) than the Seyfert 1's, which have $\Gamma > 2$ (Zdziarski et al. 1995, Gondek et al. 1996, Perola et al. 2002, Malizia et al. 2003, Beckmann et al. 2006). This is not consistent with the idea that these nuclei are identical, unless the intrinsic emission is anisotropic, being harder in the equatorial plane.

However, all accreting black hole systems (both stellar and supermassive) generally show softer intrinsic spectra at higher accretion rates (hereafter parameterised as Eddington fraction, L/L_{Edd}), e.g. Laor (2000); Remillard & McClintock (2006). Thus inclination alone is not the sole determinant of the observed spectrum, and Seyferts at different L/L_{Edd} should not be expected to have the same intrinsic emission. Here we collate estimates of black hole mass and mass accretion rate for the Seyfert 1 and 2's detected out to > 50 keV from CGRO (OSSE), BeppoSAX (PDS) and INTEGRAL (IBIS) instruments. We show that these high energy samples of Seyferts span a large range L/L_{Edd} ,

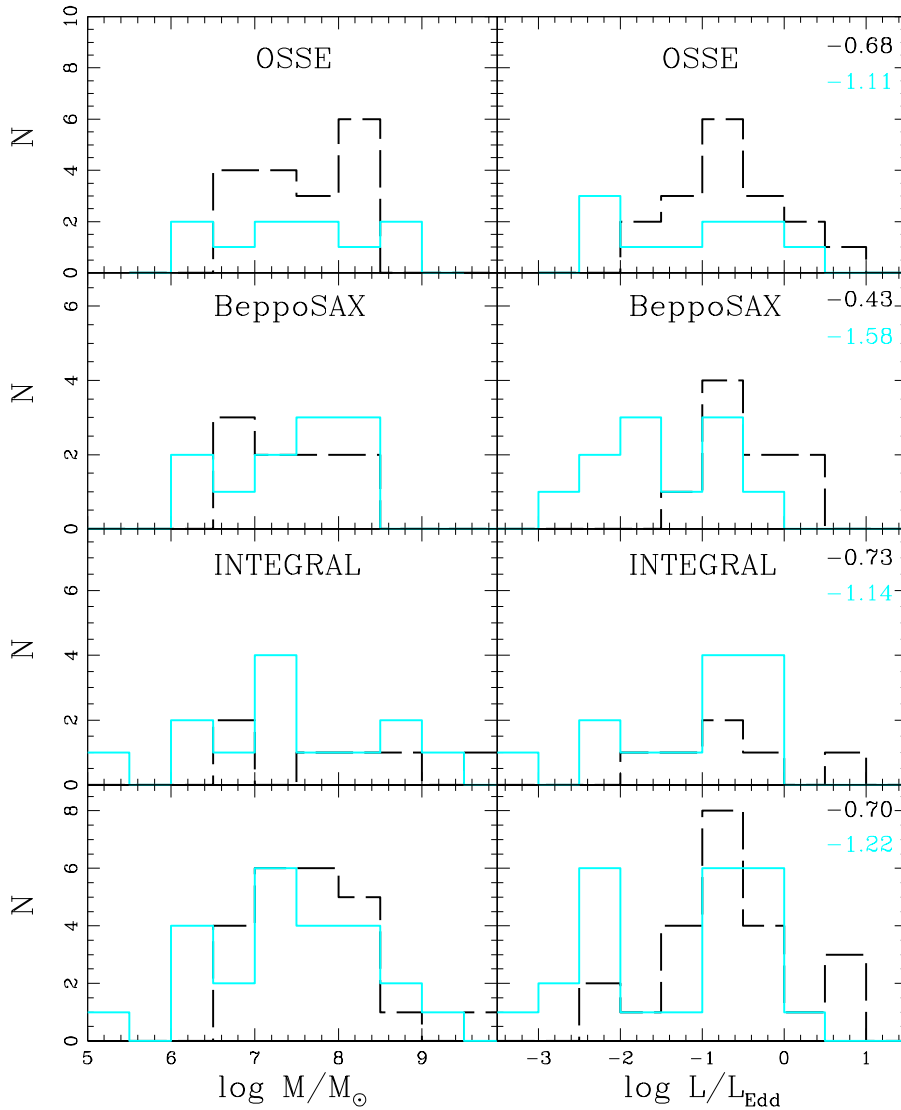


Figure 1. Plots showing the distribution of log mass and log accretion rate for individual instruments and the full sample (bottom panels) with Seyfert 1 sources shown by a black dashed line and Seyfert 2 sources by a solid cyan line. The log mean accretion rate for each type is given in the top right hand corner.

so should include a range of intrinsic spectral slopes. The mean L/L_{Edd} for the Seyfert 1's in the sample is higher than that for Seyfert 2's, consistent with the steeper spectral slope inferred for the Seyfert 1's being due to the intrinsic spectrum softening at higher L/L_{Edd} . We stress that samples of Seyfert 1 and 2 AGN need to be matched on intrinsic properties such as L/L_{Edd} in order to explore differences in orientation.

2 DATA

We construct a moderately sized sample of local hard X-ray detected AGN. These data, shown in Table 1 & 2, are taken from Malizia et al. (2003 - *BeppoSAX*), Zdziarski et al. (2000 - *OSSE*) and Beckmann et al. (2006 - *INTEGRAL*), resulting in a total sample of 47 AGN; 23 Seyfert 1s and 24 Seyfert 2s. There is always some ambiguity in assigning objects as type

1 or 2, firstly as there are optical intermediate types, and secondly as the absorption environment is complex. There is (Compton thin) molecular gas in the plane of the galaxy as well as the much smaller scale (and possibly Compton thick) molecular torus (Maiolino & Rieke 1995), and these two obscuring structures are not aligned (Nagar & Wilson 1999; Schmitt et al 2002). Thus a face on (type 1) nucleus can be obscured at both optical and X-ray wavelengths, leading to a type 2 classification (e.g. NGC 5506: Nagar et al 2002). Nonetheless, these classifications are those for which the difference in X-ray spectral index is claimed, so this is the only sample definition we can use to explore whether accretion rate can be the reason for this difference.

The black hole masses for the objects in the sample are derived primarily from stellar velocity dispersion (21 objects) and reverberation mapping (15 objects). For the remaining 11 sources the black hole masses are inferred from

Source	Instrument	logM/M _⊙	L/L _{Edd}	Reference
MCG-6-30-15	<i>OSSE</i> , <i>BeppoSAX</i> , <i>INTEGRAL</i>	6.81 ^{+0.54} _{-0.54} σ	0.25 ^x	6 (18) + 23
IC 4329A	<i>OSSE</i>	6.70 ^{+0.56} _{-peg} (mean) r	0.79 ^f	20+ 20
		6.85 ^{+0.55} _{-peg} (rms) r		
MR 2251-178	<i>INTEGRAL</i>	6.92 ^{+0.22} _{-0.22} m	4.68 ^z	10 + 21
NGC3783	<i>OSSE</i> , <i>BeppoSAX</i>	6.97 ^{+0.30} _{-0.97} (mean) r	0.23 ^f	2 + 20
		7.04 ^{+0.30} _{-0.96} (rms) r		
NGC7469	<i>OSSE</i> , <i>BeppoSAX</i>	6.81 ^{+0.30} _{-peg} (mean) r	2.14 ^f	20 + 20
		6.88 ^{+0.29} _{-peg} (rms) r		
ESO 141-55	<i>OSSE</i> , <i>BeppoSAX</i>	7.10 ^{+0.57} _{-0.57} m	2.51 ^{ox}	1
MCG-2-58-22	<i>OSSE</i>	7.14 ^{+0.57} _{-0.57} m	3.47 ^{ox}	1
NGC6814	<i>OSSE</i>	7.08 ^{+0.57} _{-0.57} r	0.05 ^f	22 + 2
3C120	<i>BeppoSAX</i>	7.36 ^{+0.22} _{-0.28} (mean) r	0.65 ^f	20 + 20
		7.48 ^{+0.21} _{-0.27} (rms) r		
NGC3516	<i>OSSE</i>	7.36 ^{+0.59} _{-0.59} r	0.07 ^f	2
Mrk279	<i>OSSE</i>	7.54 ^{+0.10} _{-0.13} r	0.13 ^z	5
NGC3227	<i>OSSE</i>	7.59 ^{+0.19} _{-peg} (mean) r	0.01 ^f	20 + 2
		7.69 ^{+0.18} _{-peg} (rms) r		
NGC5548	<i>OSSE</i> , <i>BeppoSAX</i>	8.09 ^{+0.09} _{-0.07} (mean) r	0.05 ^f	20 + 20
		7.97 ^{+0.08} _{-0.07} (rms) r		
1H 1934-063	<i>INTEGRAL</i>	7.86 ^{+0.63} _{-0.63} m	0.07 ^{ox}	1
Fairall 9	<i>BeppoSAX</i>	7.90 ^{+0.11} _{-0.31} (mean) r	0.16 ^s	20 + 20
		7.91 ^{+0.11} _{-0.32} (rms) r		
NGC7213	<i>OSSE</i>	7.99 ^{+0.64} _{-0.64} σ	0.02 ^f	2
MCG +8-11-11	<i>OSSE</i>	8.06 ^{+0.64} _{-0.64} m	0.35 ^{ox}	1
NGC526A	<i>OSSE</i> , <i>BeppoSAX</i>	8.11 ^{+0.65} _{-0.65} σ	0.17 ^{ox}	6 (18) + 1
Mrk841	<i>OSSE</i>	8.49 ^{+0.68} _{-0.68} r	0.17 ^f	22 + 2
Mrk509	<i>OSSE</i> , <i>BeppoSAX</i> , <i>INTEGRAL</i>	8.16 ^{+0.04} _{-0.04} r	0.45 ^{ox}	5 + 1
III Zw 2	<i>OSSE</i>	8.42 ^{+0.67} _{-0.67} r	0.13 ^z	3
PG 1416-129	<i>INTEGRAL</i>	8.75 ^{+0.70} _{-0.70} r	0.12 ^z	3
3C111	<i>INTEGRAL</i>	9.56 ^{+0.76} _{-0.76} m	0.01 ^z	9

Table 1. Seyfert 1 sub-sample. Name superscripts indicate the hard X-ray satellite that observed the source, o: *OSSE*, i: *INTEGRAL* & b: *BeppoSAX*. Mass superscripts refer to the measurement method, σ : stellar velocity dispersion, r: reverberation mapping, m: other. Accretion rate superscripts denote the method by which the bolometric luminosity was determined, x: correction from X-ray, f: integration of the SED flux, ox: correction from OIII, s: SED modelling, z: other. References, 1: Wang et al. (2007), 2: Woo & Urry (2002), 3: Hao et al. (2005), 4: McHardy (1988), 5: Vestergaard & Peterson. (2006), 6: Garcia-Rissmann et al. (2005), 7: Bian & Gu (2007), 8: Greenhill et al. (1997), 9: Grandi et al. (2006), 10: Morales & Fabian (2002), 11: Marconi et al. (2006), 12: Whysong & Antonucci (2004), 13: Awaki et al. (2005), 14: Czerny et al. (2001), 15: Tadhunter et al. (2003), 16: van Bemmell et al. (2003), 17: Gu et al. (2006), 18: Tremaine et al. (2002), 19: Risaliti et al. (2005), 20: Kaspil et al. (2000), 21: Monier et al. (2001), 22: Laor et al. (2001) 23: Dadina (2007). Where more than one reference is given, the first refers to the black hole mass and the second to the accretion rate. Where reference 18 is given in brackets, the relation from Tremaine et al. (2002) has been used to determine the black hole mass via stellar velocity dispersion.

optical line widths and X-ray variability measurements. For those sources with reverberation mapping measurements, the black hole mass errors quoted are those stated in the referenced literature. For the remaining sources, the quoted black hole mass errors are calculated from the relation presented in Tremaine et al. (2002).

The bolometric luminosities for the majority of the sam-

ple (22 objects) have been calculated by converting the OIII and/or X-ray luminosity to bolometric luminosity, using the relations given in Wang & Zhang (2007) and Satyapal et al. (2005) respectively. For the remaining sources, 20 have bolometric luminosities measured from the AGN SED (17 from integration of the SED & 3 from modelling) and the remaining 5 sources have bolometric luminosities stated in

Source	Instrument	$\log M/M_{\odot}$	L/L_{Edd}	Reference
NGC6300	<i>INTEGRAL</i>	5.45 $^{+0.44}_{-0.44}$ <i>m</i>	0.91 <i>x</i>	13
NGC7314	<i>BeppoSAX</i>	6.03 $^{+0.48}_{-0.48}$ σ	0.41 <i>x</i>	17 (+18)
NGC4945	<i>OSSE</i> , <i>INTEGRAL</i>	6.15 $^{+0.49}_{-0.49}$ σ	0.17 <i>x</i>	8
MCG-5-23-16	<i>OSSE</i> , <i>BeppoSAX</i>	6.29 $^{+0.50}_{-0.50}$ <i>m</i>	0.09 <i>ox</i>	1
Circinus	<i>INTEGRAL</i>	6.42 $^{+0.51}_{-0.51}$ σ	0.32 <i>ox</i>	7
NGC5506	<i>OSSE</i>	6.65 $^{+0.53}_{-0.53}$ σ	2.51 <i>ox</i>	7
NGC4593	<i>INTEGRAL</i> , <i>BeppoSAX</i>	6.91 $^{+0.55}_{-0.55}$ <i>r</i>	0.12 <i>f</i>	2
ESO 103-G35	<i>INTEGRAL</i> , <i>BeppoSAX</i>	7.14 $^{+0.57}_{-0.57}$ <i>m</i>	0.01 <i>x</i>	14
NGC4388	<i>OSSE</i> , <i>INTEGRAL</i>	7.22 $^{+0.58}_{-0.58}$ σ	0.79 <i>ox</i>	7
NGC1068	<i>INTEGRAL</i>	7.23 $^{+0.58}_{-0.58}$ σ	0.44 <i>f</i>	8 + 2
NGC7582	<i>OSSE</i>	7.25 $^{+0.58}_{-0.58}$ σ	0.35 <i>ox</i>	7
NGC5674	<i>BeppoSAX</i>	7.36 $^{+0.59}_{-0.59}$ σ	0.17 <i>x</i>	17 (+18)
ESO 323-G077	<i>INTEGRAL</i>	7.39 $^{+0.59}_{-0.59}$ <i>m</i>	0.28 <i>ox</i>	1
NGC4507	<i>OSSE</i> , <i>INTEGRAL</i>	7.58 $^{+0.61}_{-0.61}$ σ	0.27 <i>ox</i>	7
NGC4258	<i>BeppoSAX</i>	7.62 $^{+0.61}_{-0.61}$ σ	0.01 <i>f</i>	2
NGC7172	<i>OSSE</i> , <i>BeppoSAX</i>	7.67 $^{+0.61}_{-0.61}$ σ	3x10 ⁻³ <i>ox</i>	7
NGC2992	<i>BeppoSAX</i>	7.72 $^{+0.62}_{-0.62}$ σ	0.01 <i>f</i>	2
NGC5252	<i>BeppoSAX</i>	8.04 $^{+0.64}_{-0.64}$ σ	0.17 <i>s</i>	2
Centaurus A	<i>INTEGRAL</i>	8.04 $^{+0.64}_{-0.64}$ σ	7x10 ⁻⁴ <i>s</i>	11 + 12
NGC1365	<i>BeppoSAX</i>	8.18 $^{+0.65}_{-0.65}$ <i>m</i>	2x10 ⁻³ <i>x</i>	19
NGC2110	<i>OSSE</i> , <i>BeppoSAX</i>	8.30 $^{+0.66}_{-0.66}$ σ	5x10 ⁻³ <i>f</i>	2
NGC1275	<i>OSSE</i> , <i>INTEGRAL</i>	8.51 $^{+0.68}_{-0.68}$ σ	0.03 <i>f</i>	2
Mrk3	<i>OSSE</i> , <i>INTEGRAL</i>	8.65 $^{+0.69}_{-0.69}$ σ	6x10 ⁻³ <i>f</i>	2
Cyg A	<i>INTEGRAL</i>	9.40 $^{+0.75}_{-0.75}$ σ	8x10 ⁻³ <i>x</i>	15 + 16

Table 2. Seyfert 2 sub-sample. Superscripts and references as for Table 1.

the literature. The mass accretion rate is parameterized by the ratio of the bolometric luminosity to the Eddington luminosity for the given black hole mass, i.e. $\dot{M} = L_{bol}/L_{Edd}$ where $L_{Edd} = 1.3 \times 10^{38} (M_{BH}/M_{\odot})$.

Fig 1 shows the distribution of black hole mass (left panel) and Eddington fraction (right panel) for each of the high energy samples of Seyfert 1's (black, dashed line) and Seyfert 2's (cyan, solid line). It is plain that the mass accretion rates span a wide range in $L/L_{Edd} \sim 10^{-3}$ –1. This means that these AGN form a very heterogeneous sample, with the clear expectation that their high energy spectra are also heterogeneous.

The mean log mass accretion rate for each of the samples is given in the top right hand corner of the plot with Seyfert 1 in black and Seyfert 2 in red. All three instruments have higher mean L/L_{Edd} for Seyfert 1's than for the Seyfert 2's. For the complete sample we perform a series of 10,000 Monte Carlo Bootstrap simulations in order to determine rigorously the statistical significance of differences between the Seyfert 1 and Seyfert 2 distributions. The Monte Carlo Bootstrap simulations randomly select objects from the parent sample to construct paired random sub-samples (of the correct size). We then calculate the mean of the inter-

esting parameters for each randomly generated sub-sample, and the difference between these means for the sub-samples in each pair. We then measure the frequency with which our random sub-samples show differences greater than, or equal to the differences measured between the Seyfert 1 and Seyfert 2 sub-samples.

The result of the bootstrap analysis shows that the difference is significant at only $\sim 1.7\sigma$ for the combined sample, though the mean L/L_{Edd} for the Seyfert 2's and Seyfert 1's are 0.06 and 0.20, respectively. We also try to assess the systematic uncertainties in this result due to the mass determination. $H\beta$ FWHM values can give an alternative measure of black hole mass for the Seyfert 1's (e.g. Salvander et al. 2006), and we find that these are within 0.3 dex for all but one source (MR 2251-178). Removing all sources where the mass and resulting accretion rate is not found from stellar velocity dispersion or reverberation mapping (which removes MR 2251-178) reduces the significance of the difference to $<1\sigma$ due to the smaller sample size. Nevertheless, the Seyfert 1 sample still has the higher mean accretion rate (0.15 compared to 0.06 for the Seyfert 2's).

3 DISCUSSION

The X-ray spectra of stellar mass black hole binaries can be well described by a combination of emission from the accretion disc and a Comptonised tail (see e.g. the reviews by Remillard & McClintock 2006; Done, Gierlinski & Kubota 2007). The relative importance of the disc and tail can change dramatically, as does the shape of the tail, giving rise to the well known 'spectral states' as a function of (average) L/L_{Edd} . In the low/hard state, generally seen at luminosities below a few percent of Eddington, the tail dominates the X-ray emission and its spectral index is fairly well correlated with (average) mass accretion rate, with $\Gamma \sim 1.5$ at the lowest luminosities softening to $\Gamma \sim 2.1$ just before the major transition to the soft, or disc dominated states. The tail in these states can be very weak, carrying less than 20 per cent of the total bolometric power, when it has $\Gamma \sim 2.1$ (disc dominant state). Conversely, the tail can also be much stronger and softer, with $\Gamma \sim 2.5$ (very high state or steep power law state).

AGN spectra should show analogous spectral states if the properties of the accretion flow scale simply with black hole mass. There is evidence for this simple scaling, from the radio-X-ray 'fundamental plane' relations (Merloni, Heinz, & Di Matteo 2003; Falcke, Körding & Markoff 2004) and X-ray variability properties (McHardy et al. 2007; Gierlinski et al. 2007). In this picture (see e.g. Boroson 2002), LINERS, with their hard X-ray spectra and weak UV disc, are the analogues of the low/hard state (but see Maoz 2007), while Seyfert 1 and QSO's at higher L/L_{Edd} correspond to the disc dominated states, with the characteristic strong UV disc emission and consequent broad emission lines, and the Narrow line Seyfert 1's at the highest L/L_{Edd} may be the analogues of the very high state (Pounds, Done & Osborne 1995; Middleton, Done & Gierlinski 2007).

Observations of type 1 AGN spectra in the 2–10 keV band are consistent with this predicted softening of the intrinsic spectrum with increasing L/L_{Edd} (e.g. Laor 2000), so it seems highly likely that the high energy X-ray spectra considered here should also change with L/L_{Edd} . We show that current samples of Seyferts detected at high energies are clearly highly heterogeneous in this parameter (see Fig 1), so the mean spectral index will be determined by a signal-to-noise weighted average of L/L_{Edd} . The L/L_{Edd} distributions for the total Seyfert 1 and Seyfert 2 samples presented here are not significantly different (statistically) however the individual OSSE, BeppoSAX and INTEGRAL samples considered here are all consistent with having a higher mean L/L_{Edd} for the Seyfert 1's than for the Seyfert 2s. Thus, despite the limited sample size the apparently steeper spectra seen in the Seyfert 1's at high energy may be due to an intrinsic softening with increasing L/L_{Edd} . Future studies with larger samples of high energy spectra of AGN should be able to test unambiguously whether L/L_{Edd} is the major parameter in determining the shape of the 20–100 keV spectrum in Compton thin Seyferts.

REFERENCES

Antonucci R. R. J., Miller J. S., 1985, ApJ, 297, 621
 Awaki H., Kunieda H., Tawara Y., Koyama K., 1991, PASJ, 43, L37

Awaki H., Murakami H., Leighly K. M., Matsumoto C., Hayashida K., Grupe D., 2005, ApJ, 632, 793
 Bassani L., Dadina M., Maiolino R., Salvati M., Risaliti G., della Ceca R., Matt G., Zamorani G., 1999, ApJS, 121, 473
 Beckmann V., Gehrels N., Shrader C. R., Soldi S., 2006, ApJ, 638, 642
 Bian W., Gu Q., 2007, ApJ, 657, 159
 Blustin A. J., Page M. J., Fuerst S. V., Branduardi-Raymont G., Ashton C. E., 2005, A&A, 431, 111
 Boroson T. A., 2002, ApJ, 565, 78
 Cappi M., et al., 2006, A&A, 446, 459
 Czerny B., Nikolaćuk M., Piasecki M., Kuraszkiewicz J., 2001, MNRAS, 325, 865
 Dadina M., 2007, A&A, 461, 1209
 Done C., Gierlinski M., Kubota A., 2007, A&ARv, 3
 Falcke H., Körding E., Markoff S., 2004, A&A, 414, 895
 Garcia-Rissmann A., Vega L. R., Asari N. V., Cid Fernandes R., Schmitt H., González Delgado R. M., Storchi-Bergmann T., 2005, MNRAS, 359, 765
 Gondek D., Zdziarski A. A., Johnson W. N., George I. M., McNaron-Brown K., Magdziarz P., Smith D., Gruber D. E., 1996, MNRAS, 282, 646
 Grandi P., Malaguti G., Fiocchi M., 2006, ApJ, 642, 113
 Greenhill L. J., Moran J. M., Herrnstein J. R., 1997, ApJ, 481, L23
 Gu Q., Melnick J., Fernandes R. C., Kunth D., Terlevich E., Terlevich R., 2006, MNRAS, 366, 480
 Hao C. N., Xia X. Y., Mao S., Wu H., Deng Z. G., 2005, ApJ, 625, 78
 Heisler C. A., Lumsden S. L., Bailey J. A., 1997, Natur, 385, 700
 Kaspi S., Smith P. S., Netzer H., Maoz D., Jannuzi B. T., Giveon U., 2000, ApJ, 533, 631
 Laor A., 2000, NewAR, 44, 503
 Laor A., 2001, ApJ, 553, 677
 Maiolino, R., & Rieke, G. H. 1995, ApJ, 454, 95
 Malizia A., Bassani L., Stephen J. B., Di Cocco G., Fiore F., Dean A. J., 2003, ApJ, 589, L17
 Maoz D., 2007, MNRAS, 377, 1696
 Marconi A., Pastorini G., Pacini F., Axon D. J., Capetti A., Macchetto D., Koekemoer A. M., Schreier E. J., 2006, A&A, 448, 921
 McHardy I., 1988, MmSAI, 59, 239
 McHardy I., Uttley P., Taylor R., Papadakis I., 2007, ASPC, 360, 85
 Merloni A., Heinz S., di Matteo T., 2003, MNRAS, 345, 1057
 Middleton M., Done C., Gierlinski M., 2007, MNRAS, 877
 Monier E. M., Mathur S., Wilkes B., Elvis M., 2001, ApJ, 559, 675
 Morales R., Fabian A. C., 2002, MNRAS, 329, 209
 Nagar N. M., Wilson A. S., 1999, ApJ, 516, 97
 Nagar N. M., Oliva E., Marconi A., Maiolino R., 2002, A&A, 391, L21
 Nandra K., Pounds K. A., 1994, MNRAS, 268, 405
 Perola G. C., Matt G., Cappi M., Fiore F., Guainazzi M., Maraschi L., Petrucci P. O., Piro L., 2002, A&A, 389, 802
 Pounds K. A., Done C., Osborne J. P., 1995, MNRAS, 277, L5
 Remillard R. A., McClintock J. E., 2006, ARA&A, 44, 49
 Risaliti G., Elvis M., Fabbiano G., Baldi A., Zezas A., 2005, ApJ, 623, L93
 Risaliti G., Elvis M., Nicastro F., 2002, ApJ, 571, 234
 Salvander S., Shields G. A., Gebhardt K., Bonning E. W., 2006, NewAR, 50, 803
 Satyapal S., Dudik R. P., O'Halloran B., Gliozzi M., 2005, ApJ, 633, 86
 Schmitt H. R., Pringle J. E., Clarke C. J., Kinney A. L., 2002, ApJ, 575, 150
 Smith D. A., Done C., 1996, MNRAS, 280, 355

- Tadhunter C., Marconi A., Axon D., Wills K., Robinson T. G., Jackson N., 2003, MNRAS, 342, 861
- Turner T. J., George I. M., Nandra K., Mushotzky R. F., 1997, ApJS, 113, 23
- Tran H. D., 1995, ApJ, 440, 565
- Tremaine S., et al. , 2002, ApJ, 574, 740
- Wang J.-M., Zhang E.-P., 2007, ApJ, 660, 1072
- Whysong D., Antonucci R., 2004, ApJ, 602, 116
- Woo J.-H., Urry C. M., 2002, ApJ, 579, 530
- van Bemmell I. M., Vernet J., Fosbury R. A. E., Lamers H. J. G. L. M., 2003, MNRAS, 345, L13
- Vestergaard M., Peterson B. M., 2006, ApJ, 641, 689
- Zdziarski A. A., Johnson W. N., Done C., Smith D., McNaron-Brown K., 1995, ApJ, 438, L63
- Zdziarski A. A., Poutanen J., Johnson W. N., 2000, ApJ, 542, 703